Fidelity of the Estimation of the Deformation Gradient From Data Deduced From the Motion of Markers Placed on a Body That is Subject to an Inhomogeneous Deformation Field

Vít Průša
Faculty of Mathematics and Physics,
Charles University in Prague,
Sokolovská 83,
Praha, CZ 18675, Czech Republic
e-mail: prusv@karlin.mff.cuni.cz

K. R. Rajagopal[1]
Texas A&M University,
Department of Mechanical Engineering,
3123 TAMU,
College Station, TX 77843-3123
e-mail: krajagopal@tamu.edu

U. Saravanan
Department of Civil Engineering,
Indian Institute of Technology Madras,
Tamil Nadu,
Chennai 600036, India
e-mail: saran@iitm.ac.in

Practically all experimental measurements related to the response of nonlinear bodies that are made within a purely mechanical context are concerned with inhomogeneous deformations, though, in many experiments, much effort is taken to engender homogeneous deformation fields. However, in experiments that are carried out in vivo, one cannot control the nature of the deformation. The quantity of interest is the deformation gradient and/or its invariants. The deformation gradient is estimated by tracking positions of a finite number of markers placed in the body. Any experimental data-reduction procedure based on tracking a finite number of markers will, for a general inhomogeneous deformation, introduce an error in the determination of the deformation gradient, even in the idealized case, when the positions of the markers are measured with no error. In our study, we are interested in a quantitative description of the difference between the true gradient and its estimate obtained by tracking the markers, that is, in the quantitative description of the induced error due to the data reduction. We derive a rigorous upper bound on the error, and we discuss what factors influence the error bound and the actual error itself. Finally, we illustrate the results by studying a practically interesting model problem. We show that different choices of the tracked markers can lead to substantially different estimates of the deformation gradient and its invariants. It is alarming that even qualitative features of the material under consideration, such as the incompressibility of the body, can be evaluated differently with different choices of the tracked markers. We also demonstrate that the derived error estimate can be used as a tool for choosing the appropriate marker set that leads to the deformation gradient estimate with the least guaranteed error. [DOI: 10.1115/1.4023629]

1 Introduction

Developing constitutive relations for the nonlinear response undergone by solid bodies requires accurate experimental determination of the deformation gradient that is undergone by the body. It is commonly accepted that the distribution of the actual boundary traction is not known with a sufficient degree of accuracy point-wise, and the total load applied on the boundary is only accessible in ex vivo experimental measurement. On the other hand, the conventional wisdom is that the determination of the gradient of the deformation field from experimental data can be achieved with a sufficient degree of accuracy. Mathematically, by knowing the value of the function at different points, however many, one cannot say anything about the value of the derivative of this function at any point without making additional assumptions. This investigation examines the reasonableness of some of the commonly made assumptions to estimate the gradient of the displacement from the measured displacement and shows that the errors in some of the estimates of the gradient could be unacceptably large for these assumptions. Though this result is to be expected from a theoretical standpoint, the enormity of the error in estimating the gradients of the deformation, especially in the case of large deformations and certain commonly adopted procedures for estimating the gradient of the deformation, is what is surprising and totally contrary to conventional wisdom.

In many experiments within a purely mechanical context, wherein the body undergoes large deformations, the deformation field is determined by tracking a finite number of points, called markers, which, when imaged, show up in contrast with the body. Reports of such determination of the deformation field, especially for soft tissues, abound (see, for example, Refs. [1–18]). In many cases, such as inflation tests on arteries,[2] deformations of a beating heart, and uniaxial or biaxial deformations of a slab of inhomogeneous tissue, like those that comprise heart valves (see Ref. [18]), the underlying form of the inhomogeneous deformation field is not known. With some exceptions [5,16,19–21], invariably, a homogeneous deformation (linear deformation field) is assumed for a small subpart of the body and the corresponding principal stretch/strain invariants are computed. It is imperative to recognize that, in all these approaches, one seeks the best approximation for the deformation field (that is, the motion of the markers)

[1]Corresponding author.

Contributed by the Bioengineering Division of ASME for publication in the Journal of Biomechanical Engineering. Manuscript received September 7, 2012; final manuscript received December 28, 2012; accepted manuscript posted February 12, 2013; published online June 12, 2013. Assoc. Editor: Jeffrey W. Holmes.

[2]Saravanan et al. [14] reported that the deformation of circumflex coronary arteries does not conform to the expected deformation field. The same has been confirmed for other arteries (see Refs. [15] and [16]) also.

and not its gradient.[3] However, the quantity that is required for computing the constitutive relation is the gradient of the deformation field. This point cannot be overemphasized.

While the available experimental data, namely the coordinates associated with the position of the markers in the initial (possibly undeformed) and current (possibly deformed) configurations of the body, helps one to determine a very good approximation for the deformation field, this does not guarantee that the approximation for the deformation gradient is equally good. To show that this is indeed the case, we derive a rigorous estimate for the error in the determined deformation gradient obtained by approximating the deformation field using linear interpolation functions. We find that this error in the determination of the deformation gradient depends not only on the form of the actual deformation field that is approximated using linear interpolation functions but also on the relative positions of the markers used to find the approximating deformation field.

Since such error estimates for polynomial approximations of the deformation field are more involved and provide only an upper bound on the error, a numerical study is undertaken to determine the actual error in linear and polynomial approximations of the deformation field. The actual error is then compared with its estimate, and the sharpness of the error bound is discussed. By carrying out such a computation, we are able to demonstrate that the estimate of the gradient of the motion, and hence the estimate for the right Cauchy–Green tensor associated with an unknown inhomogeneous deformation field, is not robust when the inhomogeneous deformation field is approximated using the commonly used approximations. We also show that different approximations of the deformation field that are equally good in that they meet the allowable error that has been fixed a priori lead to significantly different results for the gradient.

To illustrate our thesis, we pick an assumed form for the inhomogeneous deformation field that is a commonly used representation for experimental data reduction that corresponds to the inflation of an incompressible right circular annular cylinder at constant length. This inhomogeneous deformation field is chosen for two reasons: The primary reason is that the assumed form for the data reduction associated with this deformation field is not a polynomial. The second reason is that this deformation is of practical interest and many investigations [15–17] have been currently devoted towards its study.

This study is concerned with the estimation of the error that creeps into the data reduction rather than in the experimental inaccuracies (noise) that would invariably be present in the determination of the coordinates of the centroid of the markers. It should be noted that, as experimental noise is always present, the errors in the data reduction will only be exacerbated by such noise.

This investigation shows that the upper bound on the error in the value of the estimated deformation gradient is enormous for one or both of the following reasons: (i) the second Fréchet derivative of the deformation field is not small and (ii) the relative position of the markers is such that it amplifies the error. Since the second Fréchet derivative of the deformation field is not small as the magnitude of the relative displacement increases for some deformations, the upper bound for the error in the estimated Frobenius norm also increases. Picking a deformation for which the second Fréchet derivative of the deformation field is not small as the magnitude of the relative displacement increases, we find that not only the error bound increases but the actual error in the Frobenius norm also tends to increase as the relative displacement becomes larger. We also show that, for two equally acceptable estimates of the deformation field, depending on the choice of markers used, the estimated Frobenius norm of the deformation gradient could differ by as much as 350%.

Even qualitative features of the deformation, like isochoricity (or lack thereof) of the deformation, cannot be determined accurately. The assumed form for the motion may meet the acceptable error norm and suggest that the motion is volume-preserving, but in reality the deformation could be nonisochoric or *vice versa*. This might be the reason for an interesting discrepancy found in the literature concerning soft biological tissues. While Tickner and Sacks [22] and Paranjothi et al. [17], who studied the deformation of the blood vessels by tracking markers, report that the blood vessels are compressible, Carew et al. [23] and Chuong and Fung [24] suggest that it is incompressible by measuring the volume of the blood vessels before and after deformation.

2 Methods

In this section, we first discuss the commonly used approximations for the deformation field and then derive an estimate for the error in the deformation gradient that is determined when the deformation field is approximated using linear interpolation function.

2.1 Methods to Estimate the Deformation Gradient. In this section, the two approximations used for estimating the deformation gradient are presented.

The first approximation uses linear functions of the form

$$x = a_0^x + a_1^x X + a_2^x Y + a_3^x Z, \quad y = a_0^y + a_1^y X + a_2^y Y + a_3^y Z, \quad z = a_0^z + a_1^z X + a_2^z Y + a_3^z Z \tag{1}$$

where a_i^j's are constants, (X, Y, Z) are the Cartesian coordinates of a typical material point in the reference configuration, and (x, y, z) are the Cartesian coordinates of the same material point in the current configuration. Knowing the location of m noncoplanar markers in the current and reference configurations, one can obtain $(a_i^x)^c$, $(a_i^y)^c$, and $(a_i^z)^c$, which is the value of a_i^x, a_i^y, and a_i^z corresponding to the *cth* choice of m markers from

$$\begin{Bmatrix} (a_0^x)^c \\ (a_1^x)^c \\ (a_2^x)^c \\ (a_3^x)^c \end{Bmatrix} = \boldsymbol{\alpha}^{-1} \begin{Bmatrix} \sum x_i \\ \sum x_i X_i \\ \sum x_i Y_i \\ \sum x_i Z_i \end{Bmatrix}, \quad \begin{Bmatrix} (a_0^y)^c \\ (a_1^y)^c \\ (a_2^y)^c \\ (a_3^y)^c \end{Bmatrix} = \boldsymbol{\alpha}^{-1} \begin{Bmatrix} \sum y_i \\ \sum y_i X_i \\ \sum y_i Y_i \\ \sum y_i Z_i \end{Bmatrix}, \quad \begin{Bmatrix} (a_0^z)^c \\ (a_1^z)^c \\ (a_2^z)^c \\ (a_3^z)^c \end{Bmatrix} = \boldsymbol{\alpha}^{-1} \begin{Bmatrix} \sum z_i \\ \sum z_i X_i \\ \sum z_i Y_i \\ \sum z_i Z_i \end{Bmatrix} \tag{2}$$

where

$$\boldsymbol{\alpha} = \begin{pmatrix} m & \sum X_i & \sum Y_i & \sum Z_i \\ \sum X_i & \sum X_i^2 & \sum X_i Y_i & \sum X_i Z_i \\ \sum Y_i & \sum X_i Y_i & \sum Y_i^2 & \sum Y_i Z_i \\ \sum Z_i & \sum X_i Z_i & \sum Y_i Z_i & \sum Z_i^2 \end{pmatrix}$$

$\sum$ denotes summation over i from 1 to m, (X_i, Y_i, Z_i) are Cartesian coordinates in the reference configuration of the *ith* marker that belongs to the m markers that have been selected, and (x_i, y_i, z_i) are the Cartesian coordinates of the same *ith* marker in the current configuration. Knowing the deformation of four markers is sufficient to find the parameters that appear in the deformation field in Eq. (1),[4] but our interest is in studying the influence of using a greater number of markers and, hence, this generalization. (Formulae in Eq. (2) correspond to the solution of the overdetermined system via the least squares method.)

[3]The terminology deformation gradient could be somewhat misleading. It refers to the gradient of the motion.

[4]The procedure for obtaining the estimate of the gradient by tracking the positions of the markers is interpreted, as it is common in the experimental mechanics community. (First, a linear approximation of the deformation field is found, and then the estimate of the deformation gradient is obtained by finding the deformation gradient of the approximated deformation field.) A mathematically inclined person would rather say that the gradient ("the tangent") at a given point is estimated by a linear fit ("a chord") of the deformation field through some adjoining points.

The second approximation that is sought for the deformation field is

$$\begin{aligned} x &= b_0^x + b_1^x X + b_2^x Y + b_3^x Z + b_4^x X^2 + b_5^x Y^2 + b_6^x Z^2 + b_7^x XY \\ &\quad + b_8^x YZ + b_9^x XZ, \\ y &= b_0^y + b_1^y X + b_2^y Y + b_3^y Z + b_4^y X^2 + b_5^y Y^2 + b_6^y Z^2 + b_7^y XY \\ &\quad + b_8^y YZ + b_9^y XZ, \\ z &= b_0^z + b_1^z X + b_2^z Y + b_3^z Z + b_4^z X^2 + b_5^z Y^2 + b_6^z Z^2 + b_7^z XY \\ &\quad + b_8^z YZ + b_9^z XZ \end{aligned} \tag{3}$$

where b_i^j's are constants. Knowing the location of ten markers in the current and reference configurations, one can obtain $(b_i^x)^c$, $(b_i^y)^c$, and $(b_i^z)^c$, which are the value of b_i^x, b_i^y, and b_i^z corresponding to the *cth* choice of ten markers through

$$\begin{Bmatrix} (b_0^x)^c \\ (b_1^x)^c \\ \vdots \\ (b_{10}^x)^c \end{Bmatrix} = \boldsymbol{\beta}^{-1} \begin{Bmatrix} x_1 \\ x_2 \\ \vdots \\ x_{10} \end{Bmatrix}, \quad \begin{Bmatrix} (b_0^y)^c \\ (b_1^y)^c \\ \vdots \\ (b_{10}^y)^c \end{Bmatrix} = \boldsymbol{\beta}^{-1} \begin{Bmatrix} y_1 \\ y_2 \\ \vdots \\ y_{10} \end{Bmatrix}, \quad \begin{Bmatrix} (b_0^z)^c \\ (b_1^z)^c \\ \vdots \\ (b_{10}^z)^c \end{Bmatrix} = \boldsymbol{\beta}^{-1} \begin{Bmatrix} z_1 \\ z_2 \\ \vdots \\ z_{10} \end{Bmatrix} \tag{4}$$

where

$$\boldsymbol{\beta} = \begin{pmatrix} 1 & X_1 & Y_1 & Z_1 & X_1^2 & Y_1^2 & Z_1^2 & X_1Y_1 & Y_1Z_1 & X_1Z_1 \\ 1 & X_2 & Y_2 & Z_2 & X_2^2 & Y_2^2 & Z_2^2 & X_2Y_2 & Y_2Z_2 & X_2Z_2 \\ \vdots & \vdots & \vdots & \vdots & \vdots & \vdots & \vdots & \vdots & \vdots & \vdots \\ 1 & X_{10} & Y_{10} & Z_{10} & X_{10}^2 & Y_{10}^2 & Z_{10}^2 & X_{10}Y_{10} & Y_{10}Z_{10} & X_{10}Z_{10} \end{pmatrix} \tag{5}$$

(X_i, Y_i, Z_i) are Cartesian coordinates in the reference configuration of the *ith* marker that belong to the ten markers that have been selected, and (x_i, y_i, z_i) are the Cartesian coordinates of the same *ith* marker in the current configuration, provided the initially selected ten markers are such that $\det(\boldsymbol{\beta}) \neq 0$.

2.2 Error in the Estimated Deformation Gradient Obtained From Linear Interpolation of the Deformation Field. Now we derive a rigorous upper bound on the norm of the difference between the gradient at point **a** and its approximation obtained by linear interpolation of function values in a neighborhood of **a**. Such an estimate will help us to quantify the error and analyze which qualitative features of the marker sets are essential for minimizing the error. Consequently, we can partially explain why different marker sets can give substantially different approximations of the gradient.

Let $\boldsymbol{\chi} : U \subset \mathbb{R}^3 \mapsto \mathbb{R}^3$ denote the deformation, and let us assume that the deformation is a sufficiently smooth function. The gradient (Fréchet derivative) at point **a** is defined as the linear mapping $\nabla\boldsymbol{\chi}(\mathbf{a}) : \mathbb{R}^3 \mapsto \mathbb{R}^3$ that satisfies

$$\lim_{|\mathbf{y}-\mathbf{a}|\to 0+} |\boldsymbol{\chi}(\mathbf{y}) - \boldsymbol{\chi}(\mathbf{a}) - [\nabla\boldsymbol{\chi}(\mathbf{a})](\mathbf{y}-\mathbf{a})| = 0 \tag{6}$$

Now we want to find an approximation of the gradient using the knowledge of the values of the deformation function at several points. If we know the values of $\boldsymbol{\chi}$ at three points $\{\mathbf{y}\}_{i=1}^3$, chosen in such a way that the points **a** and $\{\mathbf{y}\}_{i=1}^3$ are noncoplanar, then it is obvious that we can find unique linear mapping $\mathbf{L}_{\boldsymbol{\chi}}(\mathbf{a}) : \mathbb{R}^3 \mapsto \mathbb{R}^3$ such that

$$\boldsymbol{\chi}(\mathbf{y}_i) - \boldsymbol{\chi}(\mathbf{a}) - [\mathbf{L}_{\boldsymbol{\chi}}(\mathbf{a})](\mathbf{y}_i - \mathbf{a}) = \mathbf{0} \tag{7}$$

holds for all $\{\mathbf{y}\}_{i=1}^3$. Then, we can ask what can be said about the difference $\mathbf{L}_{\boldsymbol{\chi}}(\mathbf{a}) - \nabla\boldsymbol{\chi}(\mathbf{a})$, thus the difference between the gradient and its approximation at the given point **a**.

First, we will consider the simple problem of the approximation of the derivative of a scalar valued function of a single variable and then the more interesting case of the approximation of gradient of a scalar function of several variables. This will allow us to emphasize the differences between the one-dimensional and multidimensional setting. The latter case can be seen as a discussion of the error estimate for one component of mapping $\boldsymbol{\chi} : \mathbb{R}^3 \mapsto \mathbb{R}^3$. Using this result for the scalar-valued case, we finally derive an error estimate in the desired case of the vector-valued function of several variables.

2.2.1 Error Estimate in the Case of a Scalar-Valued Function of a Single Variable. The situation is simple for a scalar-valued function of a single variable, $f : \mathbb{R} \mapsto \mathbb{R}$. The well-known theorem on the remainder of the Taylor formula implies that there exists $t \in (0, 1)$ such that

$$f(x) - f(a) - \frac{\mathrm{d}f}{\mathrm{d}x}(a)(x-a) = \frac{1}{2}\frac{\mathrm{d}^2 f}{\mathrm{d}x^2}(a + t(x-a))(x-a)^2 \tag{8}$$

Let us emphasize that Eq. (8) is indeed an equality and that it follows from the Lagrange form of the remainder for the Taylor series. We also recall that the proof is based on the mean value theorem, which does not have an analog if we work with vector-valued functions (see, for example, Ref. [25]).

For fixed y, we can also find the linear fit of the function values $f(a)$ and $f(y)$. Thus, the function $g(x)$ is defined as

$$g(x) =_{\text{def}} f(a) + L_f(a)(x-a) \tag{9}$$

where $L_f(a) =_{\text{def}} (f(y) - f(a))/(y-a)$ is the estimate of the slope of f at point a, $\mathrm{d}f/\mathrm{d}x(a)$. Then, the difference $L_f(a) - \mathrm{d}f/\mathrm{d}x(a)$ can be estimated using Eq. (8) as follows:

$$\left|\frac{f(y)-f(a)}{y-a} - \frac{\mathrm{d}f}{\mathrm{d}x}(a)\right| = \left|\frac{\left(f(a) + \frac{\mathrm{d}f}{\mathrm{d}x}(a)(y-a) + \frac{1}{2}\frac{\mathrm{d}^2 f}{\mathrm{d}x^2}(a + t(y-a))(y-a)^2\right) - f(a)}{y-a} - \frac{\mathrm{d}f}{\mathrm{d}x}(a)\right|$$

$$\leq \frac{1}{2}\left|\frac{\mathrm{d}^2 f}{\mathrm{d}x^2}(a + t(y-a))\right||y-a| \tag{10}$$

The error estimate depends on two factors—the distance between y and a and the values of the second derivative on the line segment connecting the points a and y.

2.2.2 Error Estimate in the Case of a Scalar-Valued Function of Several Variables. Let $f : \mathbb{R}^3 \mapsto \mathbb{R}$, then, for all $x \in \mathbb{R}^3$, there exists $t \in (0,1)$ such that

$$f(\mathbf{x}) - f(\mathbf{a}) - [\nabla f(\mathbf{a})](\mathbf{x}-\mathbf{a}) = \frac{1}{2}\left[\nabla^2 f(\mathbf{a}+t(\mathbf{x}-\mathbf{a}))\right](\mathbf{x}-\mathbf{a},\mathbf{x}-\mathbf{a}) \tag{11}$$

where $[\nabla^2 f(\mathbf{z})](\mathbf{u},\mathbf{v})$ denotes the application of the bilinear form of the second derivatives (Hessian) evaluated at point $\mathbf{z}$ to vectors $\mathbf{u}$ and $\mathbf{v}$. This is implied again by the remainder formula for the Taylor series expansion (see, for example, Ref. [26]).

We can also find a linear functional $L_f(\mathbf{a})$ such that the function

$$g(x) =_{\text{def}} f(\mathbf{a}) + L_f(\mathbf{a})(\mathbf{x}-\mathbf{a}) \tag{12}$$

coincides with f at $\mathbf{a}$ and at three other points $\{\mathbf{y}_i\}_{i=1}^3$ noncoplanar with $\mathbf{a}$. Mapping[5] $L_f(\mathbf{a})$ is uniquely determined by the following system of equations:

$$f(\mathbf{y}_i) - f(\mathbf{a}) - L_f(\mathbf{a})(\mathbf{y}_i - \mathbf{a}) = 0 \tag{14}$$

and it provides an approximation of $\nabla f(\mathbf{a})$. The difference between the gradient $\nabla f(\mathbf{a})$ and its approximation $L_f(\mathbf{a})$ can be estimated as follows.

Theorem 1 (Error estimate for the approximation of the gradient). Let $f : \mathbb{R}^3 \mapsto \mathbb{R}$. Let $\mathbf{a} \in \mathbb{R}^3$ be an arbitrary point, let $\{\mathbf{y}_i\}_{i=1}^3 \subset \mathbb{R}^3$ be any points such that $\{\mathbf{y}_i\}_{i=1}^3$ and $\mathbf{a}$ are noncoplanar, and let f have continuous first and second Fréchet derivatives. Further, let $L_f(\mathbf{a})$ denote the linear mapping that, for all $\{\mathbf{y}_i\}_{i=1}^3$, solves the equation

$$f(\mathbf{y}_i) - f(\mathbf{a}) - L_f(\mathbf{a})(\mathbf{y}_i - \mathbf{a}) = 0 \tag{15}$$

and let $D_f(\mathbf{a}) = \nabla f(\mathbf{a})$ and $D_f^2(\mathbf{a}) = \nabla^2 f(\mathbf{a})$ denote the first and second Fréchet derivatives of f at the point $\mathbf{a}$. Then,

$$\left|L_f(\mathbf{a}) - D_f(\mathbf{a})\right| \le \frac{3}{2} \frac{1}{\left|\det\left[\frac{\mathbf{y}_1-\mathbf{a}}{|\mathbf{y}_1-\mathbf{a}|}, \frac{\mathbf{y}_2-\mathbf{a}}{|\mathbf{y}_2-\mathbf{a}|}, \frac{\mathbf{y}_3-\mathbf{a}}{|\mathbf{y}_3-\mathbf{a}|}\right]\right|} \max_{i=1,\dots,3} \max_{t\in[0,1]} \left|D_f^2(\mathbf{a}+t(\mathbf{y}_i-\mathbf{a}))\right| \max_{i=1,\dots,3} |\mathbf{y}_i - \mathbf{a}| \tag{16}$$

where

$$\det\left[\frac{\mathbf{y}_1-\mathbf{a}}{|\mathbf{y}_1-\mathbf{a}|}, \frac{\mathbf{y}_2-\mathbf{a}}{|\mathbf{y}_2-\mathbf{a}|}, \frac{\mathbf{y}_3-\mathbf{a}}{|\mathbf{y}_3-\mathbf{a}|}\right] \tag{17}$$

denotes the determinant of 3×3 matrix formed by column vectors $\mathbf{y}_i - \mathbf{a}/|\mathbf{y}_i - \mathbf{a}|$, $i = 1, \dots, 3$.

The theorem says that the error is, unlike in the one-dimensional setting, influenced by three factors—*distances* of the points $\{\mathbf{y}_i\}_{i=1}^3$ from $\mathbf{a}$, values of the *second derivatives* of f on the line segments connecting $\mathbf{a}$ and the points $\{\mathbf{y}_i\}_{i=1}^3$, and, finally, on the *quality of the basis* formed by the unit vectors $\{\mathbf{y}_i - \mathbf{a}\}_{i=1}^3$. By the quality of the basis, we mean its deviation from the orthonormal basis. Indeed, if the basis is orthonormal, then the determinant in Eq. (16)—volume of the parallelepiped formed by the vectors—is equal to one. Consequently, the error estimate is stricter than if the vectors are nearly coplanar and the determinant is close to zero.

Unfortunately, we usually do not know the second derivative of f; hence, the estimate in Eq. (16) cannot be made fully explicit. But we are not working with a purely mathematical approximation problem, where f appears "from nowhere". If we know a priori what type of material or what class of material models are considered, then we know that the unknown function f solves some evolution equation. In this case, one can hope that there exists a regularity theory for such an equation that allows one to obtain estimates on the second derivative in terms of boundary data. (For basic introduction to regularity theory, see, for example, Ref. [27].)

To prove the theorem, we need some auxiliary tools from linear algebra, namely, theorems on properties of oblique projections. The reason is that, if we want to calculate the norm,

$$\left|L_f(\mathbf{a}) - D_f(\mathbf{a})\right| = \sup_{\mathbf{u}\in\mathbb{R}^3, |\mathbf{u}|\neq 0} \frac{\left|\left(L_f(\mathbf{a}) - D_f(\mathbf{a})\right)\mathbf{u}\right|}{|\mathbf{u}|} \tag{18}$$

we have to decompose the vector $\mathbf{u}$ into the basis formed by the vectors $\{\mathbf{y}_i - \mathbf{a}\}_{i=1}^3$. This is a potentially dangerous situation, since the basis is, in general, not orthonormal and, consequently, the magnitude of the projected vectors can be very large (see Fig. 1(*a*), showing the situation in $\mathbb{R}^2$). (Vector $\mathbf{u}$ is decomposed with regard to the basis $\{\mathbf{v}_1, \mathbf{v}_2\}$.)

Let us first recall the definition of the minimal angle between subspaces. Let U, V be linear subspaces of $\mathbb{R}^n$. We say that $\theta_{\min} \in [0, \pi/2]$ is the minimal angle between U and V if

$$\cos\theta_{\min} = \max_{\substack{\mathbf{u}\in U, \mathbf{v}\in V \\ \mathbf{u}\neq\mathbf{0}, \mathbf{v}\neq\mathbf{0}}} \frac{\mathbf{u}\bullet\mathbf{v}}{|\mathbf{u}||\mathbf{v}|} \tag{19}$$

Theorem 3 (Norm of oblique projection in $\mathbb{R}^n$). Let V_1 and V_2 be complementary subspaces in $\mathbb{R}^n$; that is, $V_1 \oplus V_2 = \mathbb{R}^n$. Let $P_{\mathbb{R}^n \overset{V_1}{\mapsto} V_2}$ be an oblique projection along V_1 to V_2. Then

$$\left|P_{\mathbb{R}^n \overset{V_1}{\mapsto} V_2}\right| = \frac{1}{\sin\theta_{\min}} \tag{20}$$

where $\theta_{\min}$ is the minimal angle between V_1 and V_2.

For the proof, see, for example, Ref. [28].

Lemma 4 (Norm of oblique projection along one-dimensional subspace in $\mathbb{R}^2$). Let[6] $U = \mathcal{L}(\{\mathbf{v}_2\})$ and $V = \mathcal{L}(\{\mathbf{v}_1\})$ be complementary subspaces in $\mathbb{R}^2$. Let $P_{\mathbb{R}^2 \overset{U}{\mapsto} V}$ be an oblique projection along U to V. Then

[5] In what follows, we freely interpret $L_f(\mathbf{a})$ either as a functional or as a vector. This is acceptable in $\mathbb{R}^3$ with the standard scalar product. Further, we use the same symbol $|\cdot|$ for various norms—magnitude of a scalar, Euclidean norm of a vector, and the standard norm of a linear functional or linear operator. We recall that, if F is a functional on vector space V, then the norm of the functional is defined as $|F| = \sup_{\mathbf{v}\in V, \mathbf{v}\neq 0} \frac{|F\mathbf{v}|}{|\mathbf{v}|}$. If F is interpreted as a vector in $\mathbb{R}^3$, then one can also find its Euclidean norm and it turns out that both norms are equivalent.

[6] By $\mathcal{L}(\{\mathbf{w}\}_{i=1}^k)$, we denote the space spanned by the vectors $\{\mathbf{w}\}_{i=1}^k$.

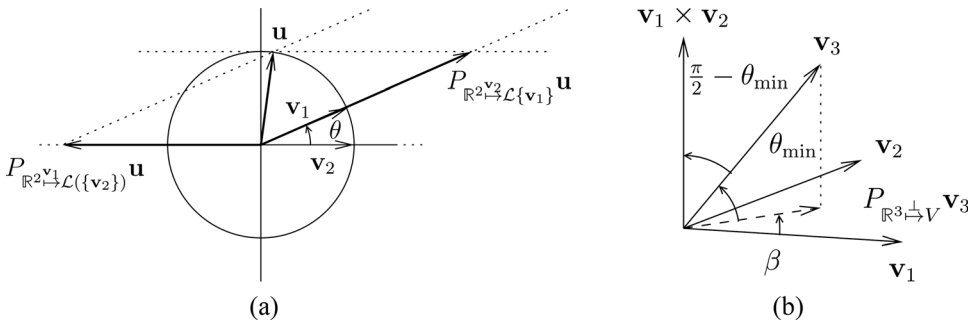

Fig. 1 Projection to a nonorthonormal basis

$$\left|P_{\mathbb{R}^2 \overset{U}{\mapsto} V}\right| = \frac{1}{\sin \beta_{\mathbf{v}_1,\mathbf{v}_2}} \tag{21}$$

where $\beta_{\mathbf{v}_1,\mathbf{v}_2}$ is the minimal angle between V_1 and V_2 and $\beta_{\mathbf{v}_1,\mathbf{v}_2}$ is given by the formula

$$\cos \beta_{\mathbf{v}_1,\mathbf{v}_2} = \frac{\mathbf{v}_1}{|\mathbf{v}_1|} \bullet \frac{\mathbf{v}_2}{|\mathbf{v}_2|} \tag{22}$$

The proof follows immediately from the definition of the minimal angle and Theorem 3.

Lemma 5 (Norm of oblique projection along one-dimensional subspace in $\mathbb{R}^3$). Let $U = \mathcal{L}(\{\mathbf{v}_3\})$ and $V = \mathcal{L}(\{\mathbf{v}_1, \mathbf{v}_2\})$ be complementary subspaces in $\mathbb{R}^3$. Let $P_{\mathbb{R}^3 \overset{U}{\mapsto} V}$ be an oblique projection along U to V. Then

$$\left|P_{\mathbb{R}^3 \overset{U}{\mapsto} V}\right| = \frac{\sin \beta_{\mathbf{v}_1,\mathbf{v}_2}}{\left|\det\left[\frac{\mathbf{v}_1}{|\mathbf{v}_1|}, \frac{\mathbf{v}_2}{|\mathbf{v}_2|}, \frac{\mathbf{v}_3}{|\mathbf{v}_3|}\right]\right|} \tag{23}$$

where $\beta_{\mathbf{v}_1,\mathbf{v}_2}$ is the minimal angle between subspaces $V_1 = \mathcal{L}(\{\mathbf{v}_1\})$ and $V_2 = \mathcal{L}(\{\mathbf{v}_2\})$ and $[\mathbf{v}_1/|\mathbf{v}_1|, \mathbf{v}_2/|\mathbf{v}_2|, \mathbf{v}_3/|\mathbf{v}_3|]$ denotes the matrix formed by normalized column vectors $\mathbf{v}_i/|\mathbf{v}_i|$, $i = 1, \ldots, 3$.

For the proof, using Theorem 3, we know that

$$\left|P_{\mathbb{R}^3 \overset{U}{\mapsto} V}\right| = \frac{1}{\sin \theta_{\min}} \tag{24}$$

where $\cos \theta_{\min} = \max_{\substack{\mathbf{u} \in U, \mathbf{v} \in V \\ \mathbf{u} \neq \mathbf{0}, \mathbf{v} \neq \mathbf{0}}} \mathbf{u} \bullet \mathbf{v}/(|\mathbf{u}||\mathbf{v}|)$. What remains to be done is to find an explicit formula for $\theta_{\min}$. The situation in $\mathbb{R}^3$ is schematically shown in Fig. 1(*b*).

Using the orthogonal projection $P_{\mathbb{R}^3 \overset{\perp}{\mapsto} V}\mathbf{v}_3$, we can find a point in V that is closest to the point given by the vector $\mathbf{v}_3$. The minimal angle $\theta_{\min}$ is then the angle between $\mathbf{v}_3$ and its orthogonal projection to $P_{\mathbb{R}^3 \overset{\perp}{\mapsto} V}\mathbf{v}_3$ to V. This can be shown as follows.

We can—without loss of generality—assume that the $V = \mathcal{L}(\{\mathbf{e}_1, \mathbf{e}_2\})$, where $\{\mathbf{e}_i\}_{i=1,2}$ are the first two canonical unit vectors in $\mathbb{R}^3$. This can be achieved by a suitable rotation of the coordinate system, and since the formula for $\theta_{\min}$ includes only scalar products and norms, it is insensitive to such a transformation. Then, any unit vector in $\mathbf{v} \in V$ can be rewritten as

$$\mathbf{v} = \begin{bmatrix} \cos \alpha \\ \sin \alpha \\ 0 \end{bmatrix} \tag{25}$$

where $\alpha \in [0, 2\pi)$ and the unit vector in U is given as

$$\mathbf{v} = \begin{bmatrix} \cos \theta \cos \varphi \\ \cos \theta \sin \varphi \\ \sin \theta \end{bmatrix} \tag{26}$$

where θ and φ are given (fixed) directional angles. Forming the scalar product in Eq. (19) yields the following one-dimensional problem

$$\begin{aligned} \cos \theta_{\min} &= \max_{\alpha \in [0,2\pi)} \begin{bmatrix} \cos \theta \cos \varphi \\ \cos \theta \sin \varphi \\ \sin \theta \end{bmatrix} \bullet \begin{bmatrix} \cos \alpha \\ \sin \alpha \\ 0 \end{bmatrix} \\ &= \cos \theta (\cos \alpha \cos \varphi + \sin \alpha \sin \varphi) \end{aligned} \tag{27}$$

The maximum is attained at point $\alpha = \varphi$, that is, when the orientation of $\mathbf{v}$ coincides with orientation of the orthogonal projection of $\mathbf{v}_3$ to V. The maximum value is $\cos \theta$, which is the magnitude of the projected vector. If we know that $\theta_{\min}$ is equal to the directional angle θ with respect to the plane determined by vectors $\mathbf{v}_1$ and $\mathbf{v}_2$, we can easily find a coordinate-free formula for computation of $\theta_{\min}$; indeed

$$\cos\left(\frac{\pi}{2} - \theta_{\min}\right) = \frac{(\mathbf{v}_1 \times \mathbf{v}_2) \bullet \mathbf{v}_3}{|\mathbf{v}_1 \times \mathbf{v}_2||\mathbf{v}_3|} = \frac{\left(\frac{\mathbf{v}_1}{|\mathbf{v}_1|} \times \frac{\mathbf{v}_2}{|\mathbf{v}_2|}\right) \bullet \frac{\mathbf{v}_3}{|\mathbf{v}_3|}}{\sin \beta_{\mathbf{v}_1,\mathbf{v}_2}} \tag{28}$$

where $\beta_{\mathbf{v}_1,\mathbf{v}_2}$ is the angle[7] between vectors $\mathbf{v}_1$ and $\mathbf{v}_2$, thus the minimal angle between subspaces $V_1 = \mathcal{L}(\{\mathbf{v}_1\})$ and $V_2 = \mathcal{L}(\{\mathbf{v}_2\})$. This concludes the proof, since $\left(\frac{\mathbf{v}_1}{|\mathbf{v}_1|} \times \frac{\mathbf{v}_2}{|\mathbf{v}_2|}\right) \bullet \frac{\mathbf{v}_3}{|\mathbf{v}_3|} = \det\left[\frac{\mathbf{v}_1}{|\mathbf{v}_1|}, \frac{\mathbf{v}_2}{|\mathbf{v}_2|}, \frac{\mathbf{v}_3}{|\mathbf{v}_3|}\right]$.

Now we are ready to prove Theorem 1.

Recall that we want to find an estimate of the norm in Eq. (18). Using the formula for the Taylor series remainder, we know that, for all $\mathbf{x} \in \mathbb{R}^3$, there exists $t \in (0, 1)$ such that

$$f(\mathbf{x}) - f(\mathbf{a}) - [D_f(\mathbf{a})](\mathbf{x} - \mathbf{a}) = \frac{1}{2}\left[D_f^2(\mathbf{a} + t(\mathbf{x} - \mathbf{a}))\right](\mathbf{x} - \mathbf{a}, \mathbf{x} - \mathbf{a}) \tag{29}$$

In particular, Eq. (29) holds for all $\{\mathbf{y}_i\}_{i=1}^3$,

$$f(\mathbf{y}_i) - f(\mathbf{a}) - [D_f(\mathbf{a})](\mathbf{y}_i - \mathbf{a}) = \frac{1}{2}\left[D_f^2(\mathbf{a} + t_i(\mathbf{y}_i - \mathbf{a}))\right](\mathbf{y}_i - \mathbf{a}, \mathbf{y}_i - \mathbf{a}) \tag{30}$$

[7]Whenever we interpret an angle between two vectors as the minimal angle in the sense of Definition 2, we assume that the vectors are oriented in such a way that the angle takes values in $[0, \pi/2]$.

(value of t is, in general, different for each $\mathbf{y}_i$.) The definition of $L_f(\mathbf{a})$ implies that

$$f(\mathbf{y}_i) - f(\mathbf{a}) - L_f(\mathbf{a})(\mathbf{y}_i - \mathbf{a}) = 0 \tag{31}$$

Subtracting the Eq. (31) from Eq. (30), we get

$$\big(L_f(\mathbf{a}) - D_f(\mathbf{a})\big)(\mathbf{y}_i - \mathbf{a}) = \frac{1}{2}\Big[D_f^2(\mathbf{a} + t_i(\mathbf{y}_i - \mathbf{a}))\Big](\mathbf{y}_i - \mathbf{a}, \mathbf{y}_i - \mathbf{a}) \tag{32}$$

Recall that we want the estimate in Eq. (16). Since $\{\mathbf{y}_i - \mathbf{a}\}_{i=1}^3$ are noncoplanar vectors, they form a basis in $\mathbb{R}^3$. For any $\mathbf{u}/|\mathbf{u}| \in \mathbb{R}^3$, we can therefore find $\{c_i\}_{i=1}^3$ such that

$$\frac{\mathbf{u}}{|\mathbf{u}|} = \sum_{i=1}^{3} c_i \frac{\mathbf{y}_i - \mathbf{a}}{|\mathbf{y}_i - \mathbf{a}|} \tag{33}$$

Moreover, we have an explicit formula for each c_i. For example, c_1 is given as

$$P_{\mathcal{L}\left(\left\{\frac{\mathbf{y}_2-\mathbf{a}}{|\mathbf{y}_2-\mathbf{a}|}, \frac{\mathbf{y}_1-\mathbf{a}}{|\mathbf{y}_1-\mathbf{a}|}\right\}\right)}^{\frac{\mathbf{y}_2-\mathbf{a}}{|\mathbf{y}_2-\mathbf{a}|}} P_{\mathcal{L}\left(\left\{\frac{\mathbf{y}_1-\mathbf{a}}{|\mathbf{y}_1-\mathbf{a}|}\right\}\right)}^{\mathbb{R}^3} P_{\mathcal{L}\left(\left\{\frac{\mathbf{y}_2-\mathbf{a}}{|\mathbf{y}_2-\mathbf{a}|}, \frac{\mathbf{y}_1-\mathbf{a}}{|\mathbf{y}_1-\mathbf{a}|}\right\}\right)}^{\frac{\mathbf{y}_3-\mathbf{a}}{|\mathbf{y}_3-\mathbf{a}|}} \frac{\mathbf{u}}{|\mathbf{u}|} = c_1 \frac{\mathbf{y}_1 - \mathbf{a}}{|\mathbf{y}_1 - \mathbf{a}|} \tag{34}$$

thus, $c_1(\mathbf{y}_1 - \mathbf{a}/|\mathbf{y}_1 - \mathbf{a}|)$ is obtained as a sequence of oblique projections. First, we project along $\mathbf{y}_3 - \mathbf{a}/|\mathbf{y}_3 - \mathbf{a}|$ to $\mathcal{L}\big(\{\mathbf{y}_2 - \mathbf{a}/|\mathbf{y}_2 - \mathbf{a}|, \mathbf{y}_1 - \mathbf{a}/|\mathbf{y}_1 - \mathbf{a}|\}\big)$ and then along $(\mathbf{y}_2 - \mathbf{a}/|\mathbf{y}_2 - \mathbf{a}|)$ to $\mathcal{L}\big(\{\mathbf{y}_1 - \mathbf{a}/|\mathbf{y}_1 - \mathbf{a}|\}\big)$. Further,

$$\begin{aligned}
|c_1| &= \left| P_{\mathcal{L}\left(\left\{\frac{\mathbf{y}_2-\mathbf{a}}{|\mathbf{y}_2-\mathbf{a}|}, \frac{\mathbf{y}_1-\mathbf{a}}{|\mathbf{y}_1-\mathbf{a}|}\right\}\right)}^{\frac{\mathbf{y}_2-\mathbf{a}}{|\mathbf{y}_2-\mathbf{a}|}} P_{\mathcal{L}\left(\left\{\frac{\mathbf{y}_1-\mathbf{a}}{|\mathbf{y}_1-\mathbf{a}|}\right\}\right)}^{\mathbb{R}^3} P_{\mathcal{L}\left(\left\{\frac{\mathbf{y}_2-\mathbf{a}}{|\mathbf{y}_2-\mathbf{a}|}, \frac{\mathbf{y}_1-\mathbf{a}}{|\mathbf{y}_1-\mathbf{a}|}\right\}\right)}^{\frac{\mathbf{y}_3-\mathbf{a}}{|\mathbf{y}_3-\mathbf{a}|}} \frac{\mathbf{u}}{|\mathbf{u}|} \right| \\
&\le \left| P_{\mathcal{L}\left(\left\{\frac{\mathbf{y}_2-\mathbf{a}}{|\mathbf{y}_2-\mathbf{a}|}, \frac{\mathbf{y}_1-\mathbf{a}}{|\mathbf{y}_1-\mathbf{a}|}\right\}\right)}^{\frac{\mathbf{y}_2-\mathbf{a}}{|\mathbf{y}_2-\mathbf{a}|}} P_{\mathcal{L}\left(\left\{\frac{\mathbf{y}_1-\mathbf{a}}{|\mathbf{y}_1-\mathbf{a}|}\right\}\right)}^{\mathbb{R}^3} P_{\mathcal{L}\left(\left\{\frac{\mathbf{y}_2-\mathbf{a}}{|\mathbf{y}_2-\mathbf{a}|}, \frac{\mathbf{y}_1-\mathbf{a}}{|\mathbf{y}_1-\mathbf{a}|}\right\}\right)}^{\frac{\mathbf{y}_3-\mathbf{a}}{|\mathbf{y}_3-\mathbf{a}|}} \right| \left| \frac{\mathbf{u}}{|\mathbf{u}|} \right| \\
&= \frac{1}{\sin\beta_{\mathbf{v}_1,\mathbf{v}_2}} \frac{\sin\beta_{\mathbf{v}_1,\mathbf{v}_2}}{\left|\det\left[\frac{\mathbf{y}_1-\mathbf{a}}{|\mathbf{y}_1-\mathbf{a}|}, \frac{\mathbf{y}_2-\mathbf{a}}{|\mathbf{y}_2-\mathbf{a}|}, \frac{\mathbf{y}_3-\mathbf{a}}{|\mathbf{y}_3-\mathbf{a}|}\right]\right|} = \frac{1}{\left|\det\left[\frac{\mathbf{y}_1-\mathbf{a}}{|\mathbf{y}_1-\mathbf{a}|}, \frac{\mathbf{y}_2-\mathbf{a}}{|\mathbf{y}_2-\mathbf{a}|}, \frac{\mathbf{y}_3-\mathbf{a}}{|\mathbf{y}_3-\mathbf{a}|}\right]\right|}
\end{aligned} \tag{35}$$

where we have used Lemma 4 and 5. Obviously, the same estimate holds also for c_2 and c_3. Now we can estimate the term in the norm given in Eq. (18),

$$\begin{aligned}
\frac{\big|\big(L_f(\mathbf{a}) - D_f(\mathbf{a})\big)\mathbf{u}\big|}{|\mathbf{u}|} &\le \sum_{i=1}^{3} |c_i| \left| \big(L_f(\mathbf{a}) - D_f(\mathbf{a})\big) \frac{\mathbf{y}_i - \mathbf{a}}{|\mathbf{y}_i - \mathbf{a}|} \right| \\
&\le \frac{1}{2} \sum_{i=1}^{3} \frac{1}{\left|\det\left[\frac{\mathbf{y}_1-\mathbf{a}}{|\mathbf{y}_1-\mathbf{a}|}, \frac{\mathbf{y}_2-\mathbf{a}}{|\mathbf{y}_2-\mathbf{a}|}, \frac{\mathbf{y}_3-\mathbf{a}}{|\mathbf{y}_3-\mathbf{a}|}\right]\right|} \frac{1}{|\mathbf{y}_i - \mathbf{a}|} \left| \Big[D_f^2(\mathbf{a} + t_i(\mathbf{y}_i - \mathbf{a}))\Big](\mathbf{y}_i - \mathbf{a}, \mathbf{y}_i - \mathbf{a}) \right| \\
&\le \frac{1}{2} \sum_{i=1}^{3} \frac{1}{\left|\det\left[\frac{\mathbf{y}_1-\mathbf{a}}{|\mathbf{y}_1-\mathbf{a}|}, \frac{\mathbf{y}_2-\mathbf{a}}{|\mathbf{y}_2-\mathbf{a}|}, \frac{\mathbf{y}_3-\mathbf{a}}{|\mathbf{y}_3-\mathbf{a}|}\right]\right|} \Big|D_f^2(\mathbf{a} + t_i(\mathbf{y}_i - \mathbf{a}))\Big| |\mathbf{y}_i - \mathbf{a}| \\
&\le \frac{3}{2} \frac{1}{\det\left[\frac{\mathbf{y}_1-\mathbf{a}}{|\mathbf{y}_1-\mathbf{a}|}, \frac{\mathbf{y}_2-\mathbf{a}}{|\mathbf{y}_2-\mathbf{a}|}, \frac{\mathbf{y}_3-\mathbf{a}}{|\mathbf{y}_3-\mathbf{a}|}\right]} \max_{i=1,\ldots,3} \max_{t\in[0,1]} \Big|D_f^2(\mathbf{a} + t(\mathbf{y}_i - \mathbf{a}))\Big| \max_{i=1,\ldots,3} |\mathbf{y}_i - \mathbf{a}|
\end{aligned} \tag{36}$$

where we have used Eqs. (32), (33), and (35).

2.2.3 Error Estimate in the Case of a Vector-Valued Function of Several Variables Let us now consider a vector-valued function of several variables, $\mathbf{f} : \mathbb{R}^3 \mapsto \mathbb{R}^3$. Applying Theorem 1 to components of $\mathbf{f}$, it is easy to derive the following error estimate.

Theorem 6 (Error estimate for the approximation of the gradient of a vector-valued function). Let $\mathbf{f} : \mathbb{R}^3 \mapsto \mathbb{R}^3$. Let $\mathbf{a} \in \mathbb{R}^3$ be an arbitrary point, let $\{\mathbf{y}_i\}_{i=1}^3 \subset \mathbb{R}^3$ be any points such that $\{\mathbf{y}_i\}_{i=1}^3$ and $\mathbf{a}$ are noncoplanar, and let $\mathbf{f}$ have continuous first and second Fréchet derivatives. Further, let $L_{\mathbf{f}}(\mathbf{a})$ denote the linear mapping that, for all $\{\mathbf{y}_i\}_{i=1}^3$, solves the equation

$$\mathbf{f}(\mathbf{y}_i) - \mathbf{f}(\mathbf{a}) - L_{\mathbf{f}}(\mathbf{a})(\mathbf{y}_i - \mathbf{a}) = \mathbf{0} \tag{37}$$

and let $D_{\mathbf{f}}(\mathbf{a}) = \nabla \mathbf{f}(\mathbf{a})$ and $D^2_{\mathbf{f}}(\mathbf{a}) = \nabla^2 \mathbf{f}(\mathbf{a})$ denote the first and second Fréchet derivatives of f at point $\mathbf{a}$. Then

$$|L_{\mathbf{f}}(\mathbf{a}) - D_{\mathbf{f}}(\mathbf{a})| \leq \frac{3}{2}\sqrt{3} m_a \left(\max_{j=1,\ldots,3} \max_{i=1,\ldots,3} \max_{t\in[0,1]} \left| D^2_{f_j}(\mathbf{a} + t(\mathbf{y}_i - \mathbf{a})) \right| \right) \tag{38}$$

where

$$m_a =_{\text{def}} \frac{1}{\left| \det \left[\frac{\mathbf{y}_1 - \mathbf{a}}{|\mathbf{y}_1 - \mathbf{a}|}, \frac{\mathbf{y}_2 - \mathbf{a}}{|\mathbf{y}_2 - \mathbf{a}|}, \frac{\mathbf{y}_3 - \mathbf{a}}{|\mathbf{y}_3 - \mathbf{a}|} \right] \right|} \max_{i=1,\ldots,3} |\mathbf{y}_i - \mathbf{a}| \tag{39}$$

$\{f_j\}_{i=1}^3$ denotes the components of $\mathbf{f}$, and $\left\{D^2_{f_j}\right\}_{i=1}^3$ stand for the second derivative of the respective components.

The theorem can be proved as follows. The system of equations in Eq. (37) can be rewritten in the form of equations for components of $\mathbf{f}$,

$$f_1(\mathbf{y}_i) - f_1(\mathbf{a}) - \left[L_{f_1}(\mathbf{a})\right](\mathbf{y}_i - \mathbf{a}) = 0 \tag{40a}$$

$$f_2(\mathbf{y}_i) - f_2(\mathbf{a}) - \left[L_{f_2}(\mathbf{a})\right](\mathbf{y}_i - \mathbf{a}) = 0 \tag{40b}$$

$$f_3(\mathbf{y}_i) - f_3(\mathbf{a}) - \left[L_{f_3}(\mathbf{a})\right](\mathbf{y}_i - \mathbf{a}) = 0 \tag{40c}$$

where $\left\{L_{f_j}(\mathbf{a})\right\}_{j=1}^3$ denotes the approximations of the gradients of the respective components. Obviously, row vectors $\left\{L_{f_j}(\mathbf{a})\right\}_{j=1}^3$ are the rows of the matrix of $L_{\mathbf{f}}(\mathbf{a})$,

$$L_{\mathbf{f}}(\mathbf{a}) = \begin{bmatrix} L_{f_1}(\mathbf{a}) \\ L_{f_2}(\mathbf{a}) \\ L_{f_3}(\mathbf{a}) \end{bmatrix} \tag{41}$$

Similarly, we can write

$$D_{\mathbf{f}}(\mathbf{a}) = \begin{bmatrix} \frac{\partial f_1}{\partial x_1}(\mathbf{a}) & \frac{\partial f_1}{\partial x_2}(\mathbf{a}) & \frac{\partial f_1}{\partial x_3}(\mathbf{a}) \\ \frac{\partial f_2}{\partial x_1}(\mathbf{a}) & \frac{\partial f_2}{\partial x_2}(\mathbf{a}) & \frac{\partial f_2}{\partial x_3}(\mathbf{a}) \\ \frac{\partial f_3}{\partial x_1}(\mathbf{a}) & \frac{\partial f_3}{\partial x_2}(\mathbf{a}) & \frac{\partial f_3}{\partial x_3}(\mathbf{a}) \end{bmatrix} = \begin{bmatrix} D_{f_1}(\mathbf{a}) \\ D_{f_2}(\mathbf{a}) \\ D_{f_3}(\mathbf{a}) \end{bmatrix} \tag{42}$$

Recall that we want to estimate the norm

$$|L_{\mathbf{f}}(\mathbf{a}) - D_{\mathbf{f}}(\mathbf{a})| = \sup_{\mathbf{u}\in\mathbb{R}^3, |\mathbf{u}|\neq 0} \frac{|(L_{\mathbf{f}}(\mathbf{a}) - D_{\mathbf{f}}(\mathbf{a}))\mathbf{u}|}{|\mathbf{u}|} \tag{43}$$

It is easy to show that, if we consider the usual Euclidean metric in $\mathbb{R}^3$, then the operator norm is equivalent to the Frobenius norm of the corresponding matrix representation,

$$|\mathbb{A}| = \left(\text{Tr}\left(\mathbb{A}\mathbb{A}^{\top}\right)\right)^{1/2} \tag{44}$$

and consequently

$$|L_{\mathbf{f}}(\mathbf{a}) - D_{\mathbf{f}}(\mathbf{a})|^2 = \sum_{j=1}^{3} |L_{f_j}(\mathbf{a}) - D_{f_j}(\mathbf{a})|^2 \tag{45}$$

The problem of estimating the error for a vector-valued function of several variables, therefore, effectively reduces to the problem of estimating the error for the components. Theorem 1 can be applied to each term in the sum in Eq. (45),

$$|L_{\mathbf{f}}(\mathbf{a}) - D_{\mathbf{f}}(\mathbf{a})|^2 \leq 3 \max_{j=1,2,3} \left(m_a \max_{i=1,2,3} \max_{t\in[0,1]} \left| D^2_{f_j}(\mathbf{a} + t(\mathbf{y}_i - \mathbf{a})) \right| \right)^2 \tag{46}$$

and Eq. (38) follows immediately.[8]

2.2.4 Illustrative Example. From the above estimate for the error in the computed deformation gradient, we find that it depends on two factors: namely, the nature of the deformation field being approximated and the relative position of the set of markers used to determine the deformation field. However, this estimate is an upper bound on the error; the actual error could be less than that given by Eq. (38). In order to understand how tight the estimate of the error given by Eq. (38) is in case of linear approximation of the deformation field and to demonstrate that use of higher order polynomials or a larger number of markers than required for a given order of the polynomial does not always result in a better estimate of the deformation gradient, the following illustrative example is studied.

Towards this end, we consider the deformation field corresponding to the inflation of an isotropic, incompressible annular cylinder at constant axial stretch to examine the fidelity in the determination of the invariants of the right Cauchy–Green tensor, $\mathbf{C}$, when a different deformation field—linear or quadratic form—is used to approximate the given deformation field and to obtain $\mathbf{C}$.

First, a deformation field that might be appropriate to describe the inflation of an isotropic, incompressible annular cylinder at constant length is assumed. If (R, Θ, Z) denote the cylindrical polar coordinates of a typical material point in the reference configuration, then the cylindrical polar coordinates of the same material point in the current configuration, (r, θ, z), is assumed to be related to (R, Θ, Z) through

$$r = \sqrt{r_o^2 - R_o^2 + R^2}, \quad \theta = \Theta, \quad z = Z \tag{47}$$

where R_o is the initial outer radius of the annular cylinder and r_o is the deformed outer radius of the annular cylinder. It is important to recognize that the deformation in an experiment of a real tissue subject to radial inflation need not be given by Eq. (47). However, this study shows that data reduction of a given marker displacement by various approximations can be widely different. Thus, Eq. (47) can be considered as just one of these approximations to the data.

The matrix components of the right Cauchy–Green tensor in Cartesian coordinates corresponding to the deformation field given by Eq. (47) are

$$\mathbf{C}^e_{\text{Cart}} = \begin{pmatrix} \left[\frac{R}{r}\cos(\Theta)\right]^2 + \left[\frac{r}{R}\sin(\Theta)\right]^2 & \left\{\left(\frac{r}{R}\right)^2 - \left(\frac{R}{r}\right)^2\right\}\cos(\Theta)\sin(\Theta) & 0 \\ \left\{\left(\frac{r}{R}\right)^2 - \left(\frac{R}{r}\right)^2\right\}\cos(\Theta)\sin(\Theta) & \left[\frac{R}{r}\sin(\Theta)\right]^2 + \left[\frac{r}{R}\cos(\Theta)\right]^2 & 0 \\ 0 & 0 & 1 \end{pmatrix} \tag{48}$$

[8]Note that t that maximizes the second derivative is, in general, different for each component of $\mathbf{f}$. This observation explains why, for a general vector valued function, it is impossible to get an equality of type 8 or 11.

Table 1 Cylindrical polar coordinates of markers in the reference configuration

Number	1	2	3	4	5	6	7	8	9	10	11	12
R	1	1	1	1	1	1	1	1	1	1	1	1
$\Theta - \pi/4$	0.2	0.2	0.2	0.1	0.1	0.1	−0.1	−0.1	−0.1	−0.2	−0.2	−0.2
$Z - L/2$	−0.1	0	0.1	−0.1	0	0.1	−0.1	0	0.1	−0.1	0	0.1
Number	13	14	15	16	17	18	19	20	21	22	23	24
R	0.9	0.9	0.9	0.9	0.9	0.9	0.9	0.9	0.9	0.9	0.9	0.9
$\Theta - \pi/4$	0.2	0.2	0.2	0.1	0.1	0.1	−0.1	−0.1	−0.1	−0.2	−0.2	−0.2
$Z - L/2$	−0.1	0	0.1	−0.1	0	0.1	−0.1	0	0.1	−0.1	0	0.1

Assuming that the markers are arranged ideally, as required in the reference configuration, their coordinates in the reference configuration are prescribed in cylindrical polar coordinates. Then, Eq. (47) is used to find the coordinates of these markers in the current configuration for some assumed values of r_o. Converting the coordinates of the markers from the cylindrical polar coordinates to Cartesian coordinates, the best approximation of the deformation given by Eq. (47) as a linear deformation field, Eq. (1), and as a quadratic deformation field, Eq. (3), are sought for the *cth* choice of n markers. For the estimated deformation field from the *cth* choice of n markers, the right Cauchy–Green tensor, $\mathbf{C}^c$, is estimated at the location (X_R, Y_R, Z_R) in the reference configuration. Then, from this estimated Cauchy–Green tensor at a given point in the reference configuration, $\mathbf{C}^c$, its three invariants,

$$J_1^c = \mathrm{Tr}(\mathbf{C}^c), \quad J_2^c = \mathrm{Tr}((\mathbf{C}^c)^{-1}), \quad J_3^c = \sqrt{\det(\mathbf{C}^c)} \tag{49}$$

are determined. Also, the exact value of these invariants for the deformation field given by Eq. (47) are determined by using

$$J_1^e = \mathrm{Tr}(\mathbf{C}^e_{\mathrm{Cart}}), \quad J_2^e = \mathrm{Tr}((\mathbf{C}^e_{\mathrm{Cart}})^{-1}), \quad J_3^e = \sqrt{\det(\mathbf{C}^e_{\mathrm{Cart}})} \tag{50}$$

where the right Cauchy–Green tensor, $\mathbf{C}^e_{\mathrm{Cart}}$, is as given in Eq. (48) and evaluated at (X_R, Y_R, Z_R) in the reference configuration, the same location at which $\mathbf{C}^c$ is evaluated. The location (X_R, Y_R, Z_R) is usually either the location of one of the markers used to estimate the deformation field or is the mean value of the coordinates of the markers used to estimate the deformation field, i.e., $(X_R, Y_R, Z_R) = (X_m, Y_m, Z_m)$, where $X_m = (X_1 + X_2 + \ldots + X_n)/n$, $Y_m = (Y_1 + Y_2 + \ldots + Y_n)/n$, and $Z_n = (Z_1 + Z_2 + \ldots + Z_n)/n$. Then, to study the correctness of the estimated value of the invariants of $\mathbf{C}$, we use a normalized error, ε_i, defined as

$$\varepsilon_i = (J_i^c - J_i^e)/J_i^e \tag{51}$$

Then, in order to examine the fidelity of the fit of the deformation field, we introduce the squared error (SE) defined through

$$\mathrm{SE} = \sum_{i=1}^{n} [(x_i^c - x_i^a)^2 + (y_i^c - y_i^a)^2 + (z_i^c - z_i^a)^2] \tag{52}$$

where (x_i^c, y_i^c, z_i^c) are the estimated coordinates of the *ith* marker from the *cth* choice of n markers, whose actual coordinates are (x_i^a, y_i^a, z_i^a).

3 Results and Discussion

Taking the undeformed outer radius, R_o, as the characteristic length scale and the length of the annular cylinder, $L = 20R_o$, the coordinates of the 24 markers used in this study are listed in Table 1. A subset of these markers is selected to find the deformation field and, subsequently, the invariants of $\mathbf{C}^c$.

Table 2 lists the sets of four markers selected to find the invariants, assuming that the deformation is linear. Also, in the same table (Table 2), the value of one of the parameters that controls the upper bound estimate of the error in the determined deformation gradient, which depends only on the relative position of the markers, namely, m_a, is tabulated. This quantity, m_a, in general, depends on which marker location is used to find the error in the deformation gradient. Hence, in Table 2, we list four values for m_a, each corresponding to a marker location where the error in the deformation gradient is evaluated. Thus, m_{ii} represents the value of m_a when the position vector of the marker - *ii* is used for the vector $\mathbf{a}$ in Eq. (39) and the position vectors of the remaining three markers (in this case, markers *i*, *iii*, and *iv*) are used for the $\mathbf{y}_1$, $\mathbf{y}_2$, and $\mathbf{y}_3$ vectors, respectively.

Table 2 Set of four markers selected to find the linear deformation field and the value of m_a defined in Eq. (39)

	Marker number				m_a			
Set identifier	*i*	*ii*	*iii*	*iv*	m_i	m_{ii}	m_{iii}	m_{iv}
Set - 1	3	11	15	23	17.4	17.4	15.5	15.5
Set - 2	2	3	11	14	0.4	0.6	6.7	0.6
Set - 3	1	6	13	18	6.6	6.6	6.5	6.5
Set - 4	1	6	22	23	9.2	6.0	3.6	3.4

Now the upper bound for the error in the deformation gradient can be determined, once the other parameter, which depends on the second Fréchet derivative of the deformation field and the region of the markers, is found. A straightforward calculation would show that the second Fréchet derivative of the deformation field, given in Eq. (47), is a monotonic function of R when its components are represented using a cylindrical polar coordinate basis. Given that all the markers used in this study are in the first quadrant (see Table 1) and, moreover, are within an angular dispersion of 0.2 rads, the Cartesian components of the second Fréchet derivative of the deformation field being studied varies monotonically over the region where the markers are present. Hence, the extremum values of the Cartesian components of the second Fréchet derivative of the deformation field being studied would occur at the marker locations themselves. Figure 2 portrays the variation of this maximum value of the absolute value of the Cartesian components of the second Fréchet derivative of the deformation field being studied with the value of r_o for the different marker sets listed in Table 2. Here, the factor 2.6 corresponds to the first decimal approximation of the constant $3\sqrt{3}/2$ that appears in the error estimate, Eq. (38). It can be concluded from Fig. 2 that the upper bound estimate of the error in the deformation gradient for a given marker set increases steeply as the deformed outer radius of the cylinder, r_o, increases. By virtue of this second Fréchet derivative of the deformation field, given by Eq. (47), being small when the displacement is infinitesimal (r_o being close to R_o), the error in the estimated first Fréchet derivative is also small, as it is bounded by a small number. Consequently, we determine the normalized error in the invariants (see Eq. (51)), since, if the components of the displacement

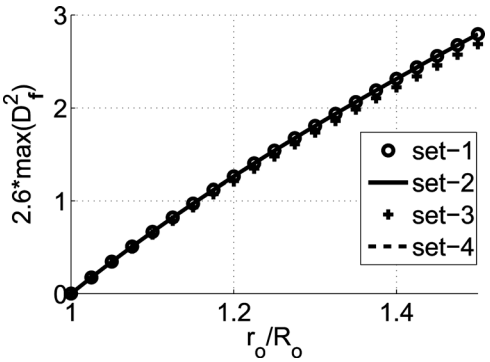

Fig. 2 Plot of the variation of 2.6 times the maximum value of the absolute value of the components of the second Fréchet derivative of the deformation given by Eq. (47) for different marker sets as a function of the deformed outer radius of the cylinder, r_o. (The values predicted by set - 1, set – 2, and set - 4 are the same.)

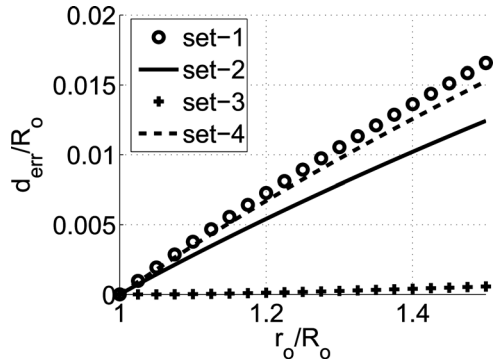

Fig. 4 Plot of the variation of the distance between the estimated and actual deformed coordinates of the point (X_m, Y_m, Z_m), d_{err}/R_o for different marker sets as a function of the deformed outer radius of the cylinder, r_o

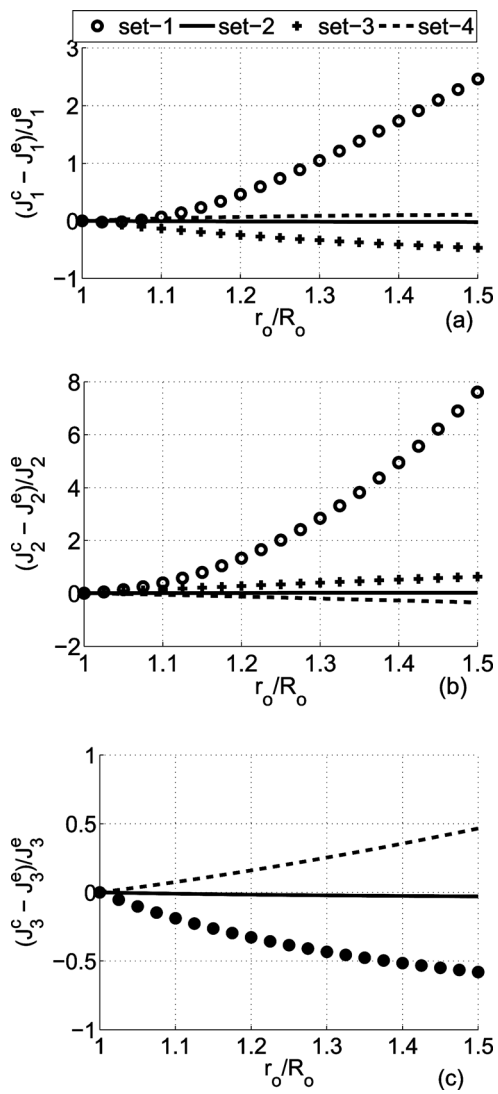

Fig. 3 Normalized error evaluated at (X_m, Y_m, Z_m) in the predicted invariants (*a*) $(J_1^c - J_1^e)/J_1^e$, (*b*) $(J_2^c - J_2^e)/J_2^e$, and (*c*) $(J_3^c - J_3^e)/J_3^e$ for different sets of four markers listed in Table 2 as a function of deformed outer radius, r_o. (Set 1 and 3 predict the same value for J_3^c.)

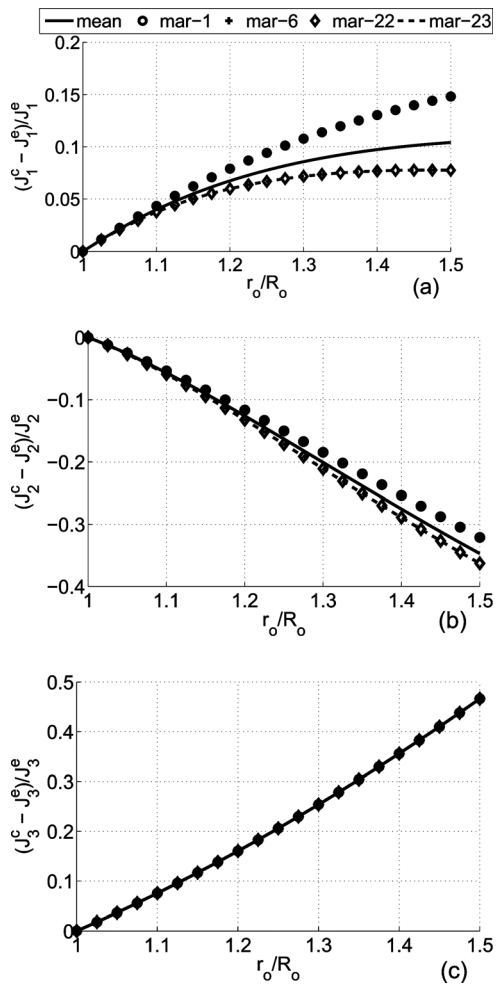

Fig. 5 Normalized error with regard to the invariants (*a*) $(J_1^c - J_1^e)/J_1^e$, (*b*) $(J_2^c - J_2^e)/J_2^e$, and (*c*) $(J_3^c - J_3^e)/J_3^e$ for the linear deformation field determined using four markers in the set - 4 listed in Table 2 at (X_m, Y_m, Z_m) and at different marker locations. (Normalized error ε_1 and ε_2 when evaluated at locations corresponding to markers 1 and 6 and corresponding to markers 22 and 23 are the same. Normalized error ε_3 is the same, irrespective of the location where it is evaluated.)

gradient are small, the error in the Frobenius norm also would tend to be a small number.

One would expect, looking at the values for m_a in Table 2, that marker set - 1 has the highest error and marker set - 2 has the least

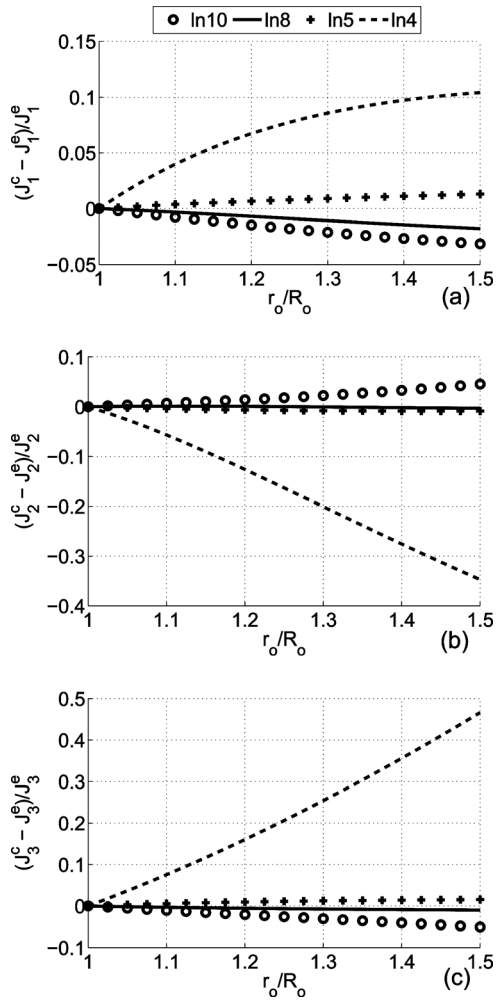

Fig. 6 Normalized error evaluated at (X_m, Y_m, Z_m) in the predicted invariants (*a*) $(J_1^c - J_1^e)/J_1^e$, (*b*) $(J_2^c - J_2^e)/J_2^e$, and (*c*) $(J_3^c - J_3^e)/J_3^e$ for different sets of markers listed in Table 4 as a function of deformed outer radius, r_o

Table 3 Error in the Frobenius norm for the set of four markers selected to find the linear deformation field listed in Table 2 when $r_o = 1.5$

	Estimated error bound				Actual error			
Identifier	*m-i*	*m-ii*	*m-iii*	*m-iv*	*m-i*	*m-ii*	*m-iii*	*m-iv*
Set - 1	48.7	48.7	43.4	43.4	9.6	9.6	9.4	9.4
Set - 2	1.1	1.7	18.8	1.7	0.01	0.01	0.01	0.2
Set - 3	18.5	18.5	18.2	18.2	1.7	1.7	1.9	1.9
Set - 4	25.8	16.8	10.1	9.5	0.6	0.6	0.3	0.3

Table 4 Variable set of markers selected to find the linear deformation field

ln10	1	3	4	6	11	18	20	21	22	23
ln8	1	4	6	11	18	21	22	23	—	—
ln5	1	6	18	22	23	—	—	—	—	—
ln4	1	6	22	23	—	—	—	—	—	—

error, since the maximum value of the second Fréchet derivative of the deformation field being studied is the same for the four marker sets studied here. Figure 3 shows that this is indeed the case. However, for marker set - 3 and marker set - 4, which have

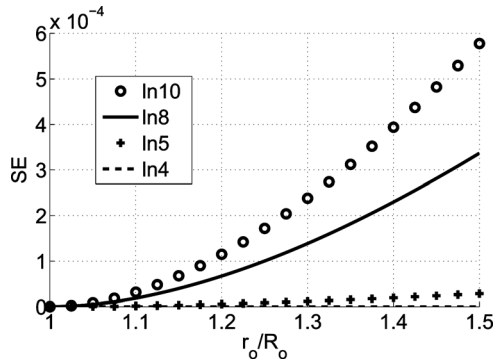

Fig. 7 Squared error (SE) for different sets of markers listed in Table 4 as a function of deformed outer radius, r_o

Table 5 Set of ten markers selected to find the deformation field

Set - 5	1	3	4	6	11	18	20	21	22	23
Set - 6	6	8	9	10	12	13	15	16	17	24
Set - 7	2	3	4	6	9	18	20	21	22	23

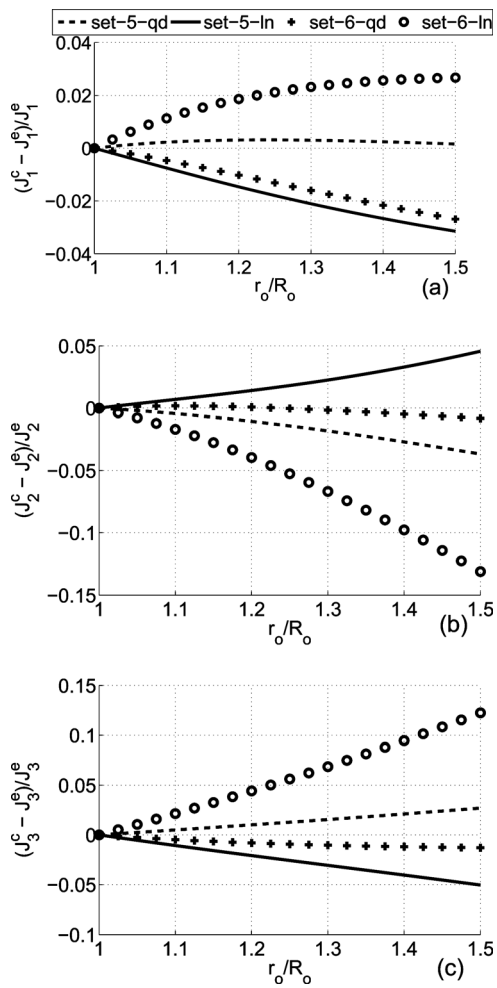

Fig. 8 Normalized error evaluated at (X_m, Y_m, Z_m) with regard to the invariants (*a*) $(J_1^c - J_1^e)/J_1^e$, (*b*) $(J_2^c - J_2^e)/J_2^e$, and (*c*) $(J_3^c - J_3^e)/J_3^e$ for different sets of ten markers listed in Table 5 and different approximations of the deformation fields, as a function of deformed outer radius, r_o

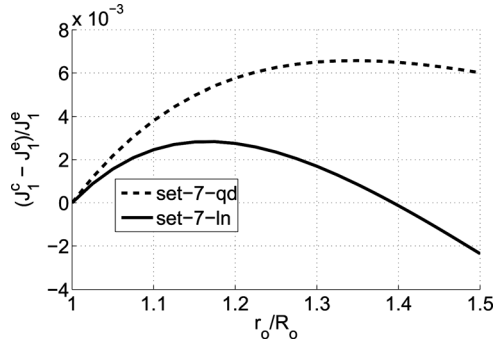

Fig. 9 Normalized error evaluated at (X_m, Y_m, Z_m) with regard to the invariant $(J_1^c - J_1^e)/J_1^e$ for set - 7 markers listed in Table 5 for different approximations of the deformation fields as a function of deformed outer radius, r_o

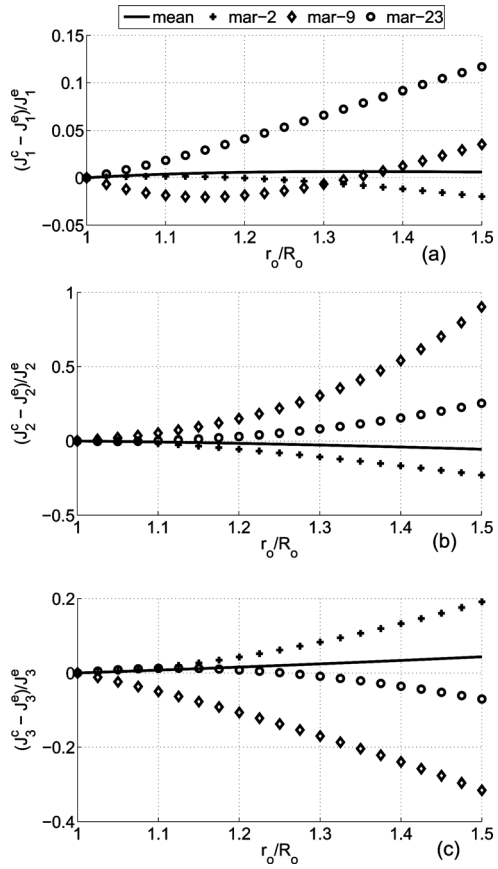

Fig. 10 Normalized error in the predicted invariants (*a*) $(J_1^c - J_1^e)/J_1^e$, (*b*) $(J_2^c - J_2^e)/J_2^e$, and (*c*) $(J_3^c - J_3^e)/J_3^e$ for quadratic deformation field determined using ten markers in set - 7 listed in Table 5 at (X_m, Y_m, Z_m) and at different marker locations

nearly half the value for m_a when compared with the marker set - 1, the actual error is no better than marker set - 1 when one considers J_3^c. This illustrates that the *error bound* should not be confused with the *actual error*.

Figure 4 portrays the distance between the estimated deformation of the point (X_m, Y_m, Z_m) and its deformation computed according to Eq. (47). That is, if (x_m^c, y_m^c, z_m^c) are the deformed coordinates of the point (X_m, Y_m, Z_m) determined from the *cth* choice of four markers and (x_m, y_m, z_m) are the actual coordinates of the same point after deformation, then

$$d_{err} = \sqrt{(x_m^c - x_m)^2 + (y_m^c - y_m)^2 + (z_m^c - z_m)^2} \tag{53}$$

It can be inferred from Fig. 4 that the error in the estimated deformation is less than 2%, while the error in the estimated deformation gradient is much higher (900%). Further, marker set – 3, which has the least error in the estimated deformation, does not have the least error in the estimated deformation gradient, proving that the markers that approximate the deformation robustly need not estimate the deformation gradient equally well.

Now let us examine the manner in which the error in the estimated deformation gradient depends on the location where it is determined. In Table 3, we tabulate the error between the estimated and the actual value of the Frobenius norm of the deformation gradient at the marker locations. In Fig. 5, the normalized error in the invariants estimated at different locations when the inhomogeneous deformation given in Eq. (47) is approximated by a linear deformation field, found using four markers in set - 2 and set - 4 (see Table 2), is portrayed as a function of increasing deformed outer radius of the cylinder. It is apparent, from these figures, that the normalized error is sensitive to the location where it is computed. While the invariants, except J_3^e, corresponding to the theoretically assumed deformation, Eq. (47), vary radially, that estimated from the linear deformation field would be constant, resulting in the normalized error to depend on the radial location where it is evaluated. By virtue of the theoretically assumed deformation, Eq. (47), being isochoric, the invariant J_3^e does not vary radially and hence, the normalized error, ε_3, is the same, irrespective of the location where it is evaluated, for the linear deformation field. Consequently, nowhere would the normalized error be zero for all the invariants.

Next, the fidelity of the estimated linear deformation field when more than four markers are used is studied. In Fig. 6, the normalized error in the estimated invariants at (X_m, Y_m, Z_m), when different numbers of markers are used to estimate the deformation field with increasing deformed outer radius of the annular cylinder, is plotted. The sets of markers used to infer the linear deformation field for the results presented in Fig. 6 are given in Table 4. It is clear from these figures that increasing the number of markers to infer the linear deformation field does not necessarily lead to an improvement in the estimated value of the invariants. However, the value of the normalized error for a particular number of markers used depends on the markers selected.

In Fig. 7, the squared error of the estimated deformation field is presented. It can be seen that, as the number of markers increases, the squared error increases. This is also to be expected because the theoretically assumed and the estimated deformation fields are different.

Now let us investigate if increasing the order of the approximating deformation field but maintaining the same number of markers improves the fidelity in the value of the estimated invariants. Towards this end, sets of ten markers listed in Table 5 are selected. The normalized error in the predicted value of the invariants for linear and quadratic deformation fields estimated using the selected ten markers as a function of increasing deformed outer radius of the annular cylinder are illustrated in Figs. 8 and 9.

It can be seen from Fig. 8 that, for a given set of n markers used, a higher order approximation of the deformation field yields better or comparable results. However, that this is a happenstance is clear from Fig. 9.

Here, it is pertinent to observe that the squared error, as defined in Eq. (52), is zero for the quadratic deformation; it increases nonlinearly to be of the order of 10^{-4} for the linear deformation, as shown in Fig. 7. Thus, this computation implies that there is no correlation between the errors in determining the theoretically assumed deformation and that of the deformation gradient, since there is no correlation between the squared error and ε_i, normalized error in the *ith* invariant, J_i.

Finally, the variation of the normalized error with the location at which it is evaluated is also studied for the quadratic deformation. Figure 10 demonstrates the variation of the normalized error with the location at which it is evaluated when the theoretically

assumed deformation, Eq. (47), is approximated by a quadratic deformation field, found using ten markers in set - 7 (see Table 5) for increasing values of the deformed outer radius of the annular cylinder. By virtue of both the estimated and theoretically assumed deformation, Eq. (47), being inhomogeneous, the normalized error's dependence on the location at which it is evaluated is complex. It can be seen from Fig. 10 that the normalized error varies both radially as well as axially and probably circumferentially too. This is because the estimated quadratic deformation field varies axially and circumferentially as well.

4 Summary and Conclusions

In Sec. 3, an inhomogeneous deformation is approximated by two deformations: one a linear deformation field and the other a quadratic deformation field, and the quality of these approximations towards the estimates of the invariants of the right Cauchy–Green tensor was explored. It was found that these estimates of the invariants from the approximations for the deformations are poor, especially as the magnitude of the deformation increases. Though this is demonstrated for a particular inhomogeneous deformation, these results are expected to hold for other inhomogeneous deformations too, as long as the assumed deformation field does not include, as a special case, the prescribed inhomogeneous deformation field.

If one knows what deformation field is to be expected, then, experimentally, that deformation field can be obtained robustly. The question that is asked and answered is whether one can estimate the gradient of the deformation and, hence, the Cauchy–Green tensor, $\mathbf{C}$, and its invariants accurately when the inhomogeneous deformation is not known. It is found that the estimated invariants are not robust through analytical error estimates as well as the actual computation of the error. Though these error estimates are not tight, they provide a rationale for selecting some marker sets over the many others that are possible theoretically to find the invariants of $\mathbf{C}$. The marker sets that result in the least value for the parameter m_a are the best suited to find the deformation gradient and, hence, the invariants of $\mathbf{C}$.

Thus, estimates of the invariants of the stretches or the nonlinear strains associated with large inhomogeneous deformations need to be interpreted with caution and engineering judgment.

Acknowledgment

The authors thank an anonymous reviewer for bringing to our attention the articles, Refs. [1,3,19]. Vít Průša thanks the Czech Science Foundation (Grant Number P101/2012/P074) for its support. U. Saravanan thanks the Department of Biotechnology, Government of India for its support. K. R. Rajagopal thanks the National Science Foundation for its support.

References

[1] Meier, G. D., Ziskin, M. C., Santamore, W. P., and Bove, A. A., 1980, "Kinematics of the Beating Heart," IEEE Trans. Biomed. Eng., **BME-27**(6), pp. 319–329.

[2] Hoffman, A. M., and Grigg, P., 1984, "A Method of Measuring Strains in Soft Tissues," J. Biomech., **17**(10), pp. 795–800.

[3] Waldman, L., Fung, Y. C., and Covell, J. W., 1985, "Transmural Myocardial Deformation in the Canine Left Ventricle: Normal *In Vivo* Three-Dimensional Finite Strains," Circ. Res., **57**, pp. 152–163.

[4] Humphrey, J. D., Vawter, D. L., and Vito, R. P., 1987, "Quantification of Strains in Biaxially Tested Soft Tissues," J. Biomech., **20**(1), pp. 59–65.

[5] Arts, T., Hunter, W. C., Douglas, A., Muijtjens, A. M. M., and Reneman, R. S., 1992, "Description of a Deformation of the Left Ventricle by a Kinematic Model," J. Biomech., **25**(10), pp. 1119–1127.

[6] May-Newman, K., and Yin, F. C., 1995, "Biaxial Mechanical Behavior of Excised Porcine Mitral Valve Leaflets," Am. J. Physiol., **269**(4), pp. H1319–H1327.

[7] O'Dell, W. C., Moore, C. C., Hunter, W. C., Zerhouni, E. A., and McVeigh, E. R., 1995, "Three-Dimensional Myocardial Deformations: Calculation With Displacement Field Fitting to Tagged MR Images," Radiology, **195**(3), pp. 829–835.

[8] Sacks, M. S., and Chuong, C. J., 1998, "Orthotropic Mechanical Properties of Chemically Treated Bovine Pericardium," Ann. Biomed. Eng., **26**, pp. 892–902.

[9] Ortt, E. M., Doss, D. J., Legall, E., Wright, N. T., and Humphrey, J. D., 2000, "A Device for Evaluating the Multiaxial Finite Strain Thermomechanical Behavior of Elastomers and Soft Tissues," ASME J. Appl. Mech., **67**(September), pp. 465–471.

[10] Greenleaf, J. F., Fatemi, M., and Insana, M., 2003, "Selected Methods for Imaging Elastic Properties of Biological Tissues," Annu. Rev. Biomed. Eng., **5**, pp. 57–78.

[11] Chen, L., Yin, F. C. P., and May-Newman, K., 2004, "The Structure and Mechanical Properties of the Mitral Valve Leaflet-Strut Chordae Transition Zone," ASME J. Biomech. Eng., **126**(April), pp. 244–251.

[12] Harris, J. L., and Humphrey, J. D., 2004, "Kinetics of Thermal Damage to a Collagenous Membrane Under Biaxial Isotonic Loading," IEEE Trans. Biomed. Eng., **51**(2), pp. 371–379.

[13] Everett, W. N., Shih, P., and Humphrey, J. D., 2005, "A Bi-plane Video-based System for Studying the Mechanics of Arterial Bifurcations," Exp. Mech., **45**(4), pp. 377–382.

[14] Saravanan, U., Baek, S., Rajagopal, K. R., and Humphrey, J. D., 2006, "On the Deformation of the Circumflex Coronary Artery During Inflation Tests at Constant Length," Exp. Mech., **46**, pp. 647–656.

[15] Genovese, K., 2009, "A Video-Optical System for Time-Resolved Whole-Body Measurement on Vascular Segments," Opt. Lasers Eng., **47**(9), pp. 995–1008.

[16] Kim, J., and Baek, S., 2011, "Circumferential Variations of Mechanical Behavior of the Porcine Thoracic Aorta During the Inflation Test," J. Biomech., **44**(10), pp. 1941–1947.

[17] Paranjothi, K., Saravanan, U., Krishnakumar, R., and Balakrishnan, K. R., 2011, "Mechanical Properties of Human Saphenous Vein," *Mechanics of Biological Systems and Materials*, T. Proulx, ed., Vol. 2, Springer, New York, pp. 79–85.

[18] Paranjothi, K., Saravanan, U., Krishnakumar, R., Balakrishnan, K. R., and Hospitals, M., 2011, "Mechanical Properties of Abnormal Human Aortic and Mitral Valves," *Mechanics of Biological Systems and Materials*, T. Proulx, ed., Vol. 2, Springer, New York, pp. 65–72.

[19] McCulloch, A. D., and Omens, J. H., 1991, "Non-homogeneous Analysis of Three-Dimensional Transmural Finite Deformations in Canine Ventricular Myocardium," J. Biomech., **24**(7), pp. 539–548.

[20] Hashima, A. R., Young, A. A., McCulloch, A. D., and Waldman, L. K., 1993, "Nonhomogeneous Analysis of Epicardial Strain Distributions During Acute Myocardial Ischemia in the Dog," J. Biomech., **26**(1), pp. 19–35.

[21] Waldman, L. K., Allen, J. J., Pavelec, R. S., and McCulloch, A. D., 1996, "Distributed Mechanics of the Right Ventricle: Effects of Varying Preload," J. Biomech., **29**(3), pp. 373–381.

[22] Tickner, E. G., and Sacks, A. H., 1967, "A Theory for the Static Elastic Behavior of Blood Vessels," Biorheology, **4**, pp. 151–168.

[23] Carew, T. E., Vaishnav, R. N., and Patel, D. J., 1968, "Compressibility of the Arterial Wall," Circ. Res., **23**, pp. 61–68.

[24] Chuong, C. J., and Fung, Y. C., 1984, "Compressibility and Constitutive Equation of Arterial Wall in Radial Compression Experiments," J. Biomech., **17**(1), pp. 35–40.

[25] McLeod, R. M., 1964, "Mean Value Theorems for Vector-Valued Functions," Proc. Edinburgh Math. Soc., **14**, pp. 197–209.

[26] Lang, S., 1997, *Undergraduate* Analysis, 2nd ed., (Undergraduate Texts in Mathematics), Springer-Verlag, New York.

[27] Evans, L. C., 1998, *Partial Differential Equations*, Vol. 19, (Graduate Studies in Mathematics), American Mathematical Society, Providence, RI.

[28] Meyer, C., 2000, *Matrix Analysis and Applied Linear Algebra*, Society for Industrial and Applied Mathematics (SIAM), Philadelphia, PA.